

# Post-processing techniques for locally self-assembled silicon nanowires

Ongi Englander<sup>a,\*</sup>, Dane Christensen<sup>a</sup>, Jongbaeg Kim<sup>b</sup>, Liwei Lin<sup>a</sup>

<sup>a</sup> *Berkeley Sensor & Actuator Center, University of California, Berkeley, CA 94720, USA*

<sup>b</sup> *School of Mechanical Engineering, Yonsei University, Seoul, South Korea*

Received 23 February 2006; received in revised form 8 July 2006; accepted 11 August 2006

Available online 15 September 2006

## Abstract

Post-processing techniques are applied after the integration and assembly of nanostructures and Microelectromechanical Systems (MEMS) to realize integrated Nanoelectromechanical Systems (NEMS). Experimentation is focused specifically on the application of post-processing steps to a locally self-assembled micro-to-nano system comprising of suspended silicon nanowires between two MEMS bridges. Local contact metallization, global metallization for rapid system functionalization and the application of aqueous treatment to the NEMS are among the post-processing techniques studied. These techniques are evaluated for their effectiveness and compatibility with integrated NEMS and traditional MEMS processes. It is found that local and global contact metallization techniques effectively alleviate inherent problems at the nano-to-micro contact and the aqueous treatment study confirms the effectiveness of the super critical drying process for nanostructures.

© 2006 Elsevier B.V. All rights reserved.

**Keywords:** NEMS; Silicon nanowires; Integration; Post-processing

## 1. Introduction

Nanoscale and NEMS based applications and devices have shown significant promise for a wide range of applications with improved performance and reduced costs when compared to their microscale counterparts [1,2]. Post-processing techniques are indispensable steps toward the functionalization, realization and operation of NEMS devices, such as chemical and mechanical sensors, biomedical detectors, electrical interconnects and switches. We explore various post-processing techniques for self-assembled and suspended silicon nanowires between two MEMS bridges, including (1) local contact metallization, (2) global metallization for rapid system functionalization and (3) aqueous treatment [3]. The self-assembled NEMS devices were previously developed using localized synthesis and electric-field assisted self-assembly of silicon nanowires with MEMS structures to yield a two-terminal NEMS device [4,5]. In contrast to more traditional approaches for integrated nanoscale applications [1,6,7], the utilization of localized heating and thus localized nanostructure synthesis permits the formation of the nano-to-micro contact in situ yielding a CMOS compatible

platform for NEMS fabrication and functionalization. Here we present our NEMS' responses to various post-processing steps where the selection of these processes focused on minimizing the complexity of the post-processing step and seeking compatibility with conventional processes. The benefits and impact of these processes are evaluated and hydrogen sensing capabilities using this post-processed NEMS are presented as a demonstration.

## 2. Experimental

The NEMS studied in this work is fabricated following a previously presented process [4,5]. The two-terminal, self-assembled silicon nanowires based system is schematically illustrated in Fig. 1. Briefly, two suspended MEMS bridges are positioned in close proximity to each other and the synthesis of silicon nanowires using the VLS growth mechanism is initiated locally as a result of the resistive heating of the hot growth bridge. In the presence of a locally acting electric-field, constructed solely between the two bridges, the silicon nanowires follow electric-field lines and link together the two MEMS bridges. The first bridge on which the nanowire synthesis process originates is designated as the growth structure while a second bridge, located nearby, is designated as the bias structure. Post-processing techniques are required to enable and improve the functionality of this NEMS device.

\* Corresponding author. Tel.: +1 510 393 4667.

E-mail address: [oenglander@gmail.com](mailto:oenglander@gmail.com) (O. Englander).

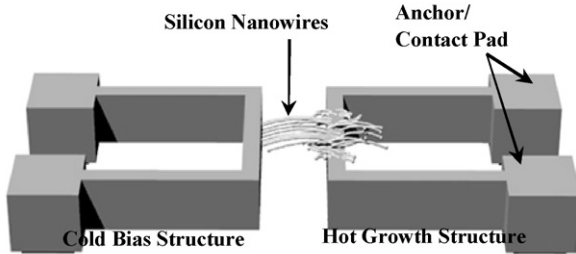


Fig. 1. Schematic of the integrated micro-to-nano system using silicon nanowires to link together two MEMS structures to yield a two-terminal NEMS by means of localized synthesis and electric-field assisted self-assembly.

Electrically unreliable contacts and high contact resistances frequently plague nanostructure-based systems. In fact, the nature of contact resistances, specifically in conjunction with lightly doped or undoped nanowires is poorly understood [8,9]. Here, we specifically address a contact formed between the highly doped silicon (MEMS bridge), close to the metallic limit, and an undoped silicon (the nanowire). We have come to expect rather mediocre electrical properties at the micro-to-nano contact particularly as our assembly method may contribute to higher resistances than do more conventional assembly processes. More specifically, while traditional post-synthesis assembly methods strive to maximize the micro-to-nano contact area, by using e-beam techniques to define relatively large contact pads as resistance is inversely proportional to area, in our process the contact area is defined by the diameter of the nanowire and hence is considerably smaller than traditionally assembled devices. In an attempt to mitigate these inherent difficulties, a localized metallization step, or a ‘patch’ step was performed following the NEMS self-assembly process. More specifically, in order to improve the electrical properties at the micro-to-nano contact, localized platinum deposition was performed using an in situ SEM deposition tool (gas injection system). While not a commonly used microscale processing tool, the in situ SEM metal deposition approach permits a quick, highly accurate, and flexible localized deposition without the requirement of any lithography steps. It has proved useful for mask repair and nonplanar surface patterning [10,11] and here enables a quick and controlled evaluation of transport properties of our micro-to-nano contacts. Approximately 20–40-nm thick platinum of various cross-sections was deposited locally along the MEMS structures at locations where the nanowires contact the MEMS structures. The localization of the Pt deposition to the respective MEMS structure was verified using an EDX tool and thus ensured that the Pt deposition regions are indeed isolated from each other and eliminated crosstalk concerns that may occur in a global deposition environment. A few examples of the localized Pt deposition are illustrated in Fig. 2. In Fig. 2(a), the localized Pt deposition is seen at the nano-to-micro contact at both the growth and bias structures. In the case of the growth structure (top of the figure), where the exact location of the nano-to-micro contact is difficult to place (typically in dense growth regions), a wider deposition area is utilized and the pres-

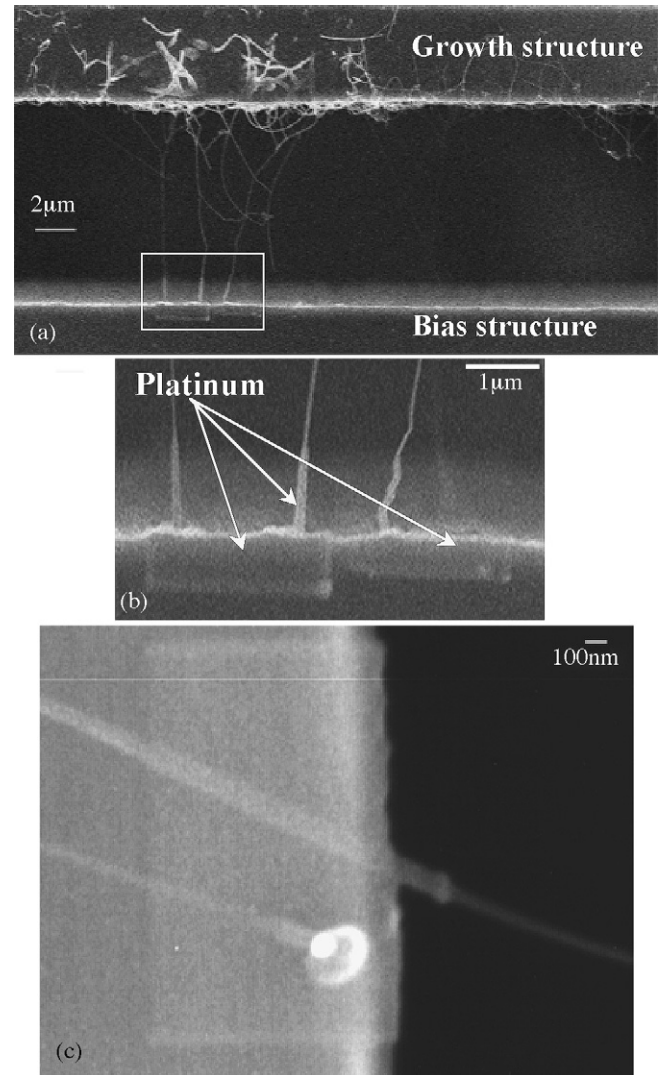


Fig. 2. Nano-to-micro contact regions following the localized platinum deposition process. (a) Localized deposition along both MEMS structures. (b) Enlarged view of marked area in (a) showing the localized platinum deposition area along the bias bridge. (c) Close-up view of an isolated  $2.3 \mu\text{m} \times 1.7 \mu\text{m}$  platinum patch and the now extended nano-to-micro contact area from a different sample.

ence of platinum deposition is evident by the larger and brighter appearing nanowires. Fig. 2(b) shows a close-up view of the bias structure in Fig. 2(a) and two slightly raised rectangular regions mark the localized deposition regions. The left-hand side region spans approximately  $2 \mu\text{m}$  in length and  $1 \mu\text{m}$  in width. Fig. 2(c) illustrates an enlarged view of the nano-to-micro contact region and a  $90 \text{ nm}$  diameter silicon nanowire is seen to increase in diameter to approximately  $130 \text{ nm}$  evident as the deposition region extends slightly into the gap. The nano-to-micro contact is clearly observed and the boundary of the  $2.3 \mu\text{m} \times 1.7 \mu\text{m}$  deposition region is clearly defined. About  $1\text{-}\mu\text{m}$  long section of the silicon nanowire is covered with platinum near the contacts. The total length of the intrinsic silicon nanowire is about  $10 \mu\text{m}$  with estimated resistance of  $4.7 \times 10^{12} \Omega$  using a resistivity of  $3 \times 10^5 \Omega \text{ cm}$  and diameter of  $90 \text{ nm}$ . The contribution of the two  $1\text{-}\mu\text{m}$  long platinum deposition regions is  $19 \Omega$  using a resistivity of  $1.05 \times 10^{-7} \Omega \text{ m}$  and estimated platinum cross sectional

area of  $5.6e3 \text{ nm}^2$ . As a result, the overall nanowire resistance obtained by adding two parallel platinum resistors at both ends of the silicon nanowire, without consideration of the nature of the nano-to-micro contacts, is reduced by approximately 20%. In order to determine the role of the platinum patch in transport properties of the system, the electrical characteristics of the NEMS are evaluated before and after the localized deposition process as discussed in the following section.

In another approach, a global metallization process was tested as a method for rapid system functionalization. Here, the global metallization step was achieved via the mask-less thermal evap-

oration of 20 nm of palladium onto the as-assembled system. While many metals are compatible with the system, palladium is chosen as it is suitable for hydrogen sensing applications [12]. While the nature of the localized deposition approach ensures that no spurious connections form between the two MEMS structures, the utilization of the global deposition approach required additional vigilance. As such, the thickness of the metallization layer was optimized to enable experimentation with sensing applications while maintaining the individual entity of each nanowire and preventing crosstalk or electrical shorts through or around the MEMS structures or the substrate (as described in Ref. [4], the MEMS structures are isolated from the substrate with a  $2 \mu\text{m}$  thick oxide). Experimentation suggests that the deposition of 20 nm of palladium onto the self-assembled NEMS would adequately meet the goals of this post-processing step. Fig. 3 shows the NEMS before and after the global palladium deposition process. The mechanical integrity of the self-assembled system appears to be preserved after the deposition process as the micro-to-nano contacts remain intact (Fig. 3(c)). The expected increase in nanowire diameter of approximately 40 nm is also observed and is consistent with the deposition thickness.

The integrity of the NEMS was further evaluated by subjecting the system to an aqueous treatment, a key component in the functionalization of nanostructures for biological sensing applications [7,13]. This post-processing step evaluated the ability of a device constructed from suspended nanostructures to withstand exposure to an aqueous environment. The experiment involved covering the NEMS along with its surroundings with a few milliliters of a low surface tension liquid, isopropyl alcohol

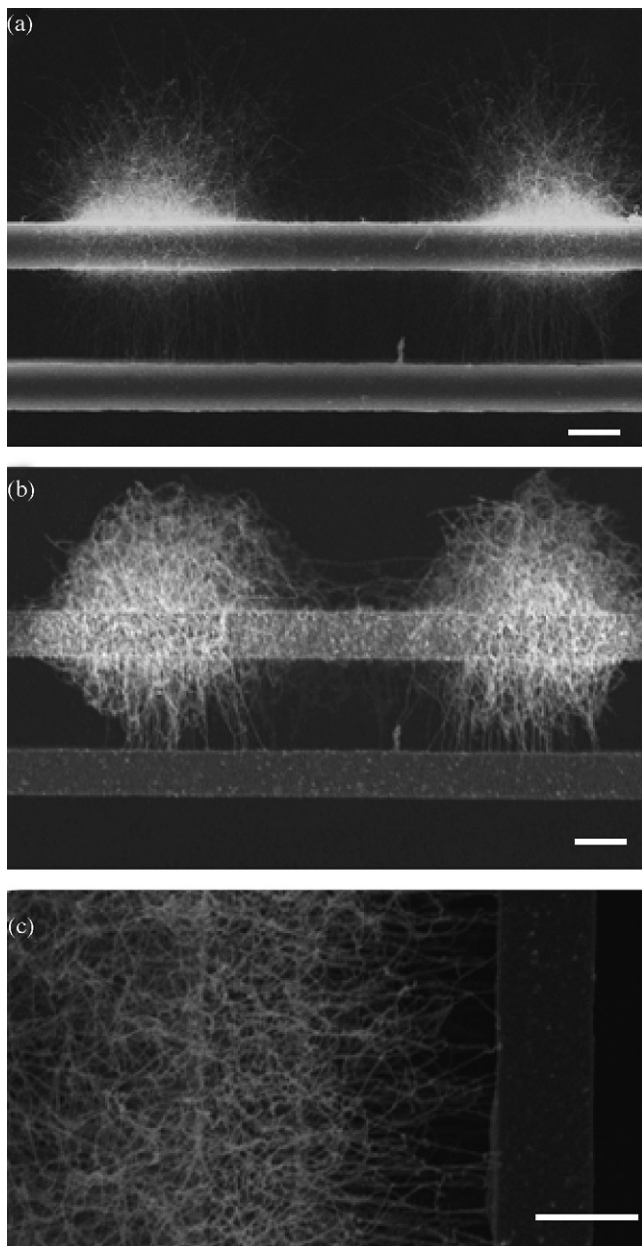


Fig. 3. (a) As-assembled NEMS (the growth structure is the top structure). (b) NEMS following the global deposition of 20 nm of palladium for hydrogen sensing applications. (c) A close-up view of the nanowires' contact to the bias structure (right) after the palladium deposition; multiple contacts are observed (scale bars are  $5 \mu\text{m}$ ).

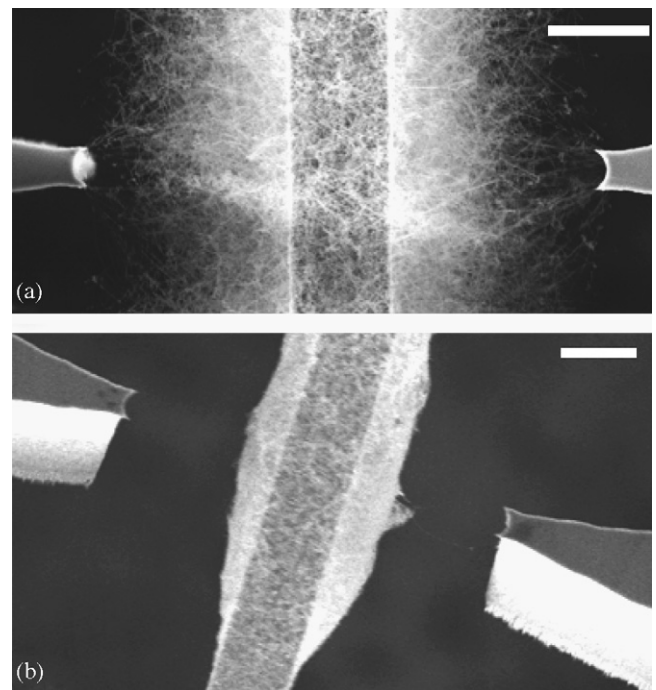


Fig. 4. (a) As-assembled NEMS (the growth structure is the center structure). (b) NEMS after exposure to an aqueous environment followed by air drying resulting in nanowires slumping over the growth structure. The loss of contact to bias structure (left and right) is evident (scale bars are  $5 \mu\text{m}$ ).

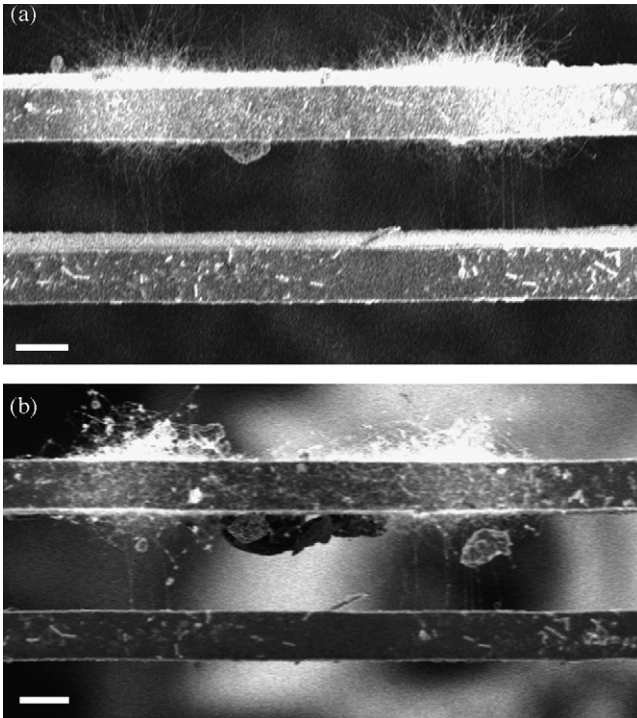


Fig. 5. (a) As-assembled NEMS (the growth structure is the top structure). (b) NEMS after exposure to an aqueous environment followed by a CPD step. There are no nanowires slumping over the MEMS structure and contacts to the bias structure remain intact. Debris introduced during the CPD process is deposited onto the system; however the nanowires and the nano-to-micro contacts remain undisturbed even with the introduction of these foreign materials (scale bars are 5  $\mu\text{m}$ ).

(IPA), followed by an accelerated drying step in air inside a 90 °C oven. Fig. 4 illustrates the NEMS response to this treatment. It appears that strong surface tension forces make the well-distributed nanowires coalesce together and break most of the nano-to-micro contacts. The appearance of a fatter growth structure in Fig. 4(b) is a result of surface tension effects which force all nanowires, throughout their length, to hang down around the growth structure. However, by following the aqueous treatment step with a critical point drying step (CPD), it is possible to ensure that most nano-to-micro contacts survive the post-processing treatment as seen in Fig. 5.

### 3. Results and discussion

The exposure of this self-assembled NEMS to various post-processing steps provides us with considerable information about the system and its characteristics. Fig. 6 shows the  $I$ - $V$  characteristics of the two-terminal NEMS before and after the localized platinum contact metallization. This set of measurements was taken from a system of only two interconnected nanowires with similar deposition characteristics as illustrated in Fig. 2. The resistance to current flow in the system is comprised of the high resistance nanowires as well as the contact resistance at each nano-to-micro interface. Since the localized Pt deposition was isolated to the contact region, the improvement in the current carrying capacity of the NEMS following

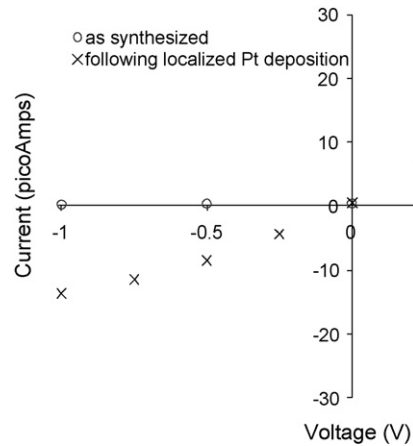


Fig. 6.  $I$ - $V$  characteristics of the NEMS before and after the localized platinum metallization process.

the localized platinum deposition may be attributed to resistance reduction at the contacts. More specifically, the resistance reduction contribution from platinum deposition into the nanowire is only about 20% without consideration of effects on the contacts while experimental results clearly shows orders of magnitude of improvement. The high contact resistances are at least partially attributed to the small contact area between the nanowires and the MEMS structures and hence the localized deposition at the contacts assists in increasing the contact area. Following the localized contact metallization, the electrical characteristics show an up to 30 pA improvement in the current carrying capacity of the NEMS under an input voltage of 1 V. The measurements were conducted using an Agilent 4155 parameter analyzer with fA resolution. The nonlinearity of the  $I$ - $V$  characteristics, however, suggests the presence of a non-ohmic contact. The non-ideal electrical behavior is expected as intrinsic silicon nanowires contact the silicon MEMS structures which are highly doped. Further improvement can be realized by adding a dopant source during the nanowire synthesis process.

While the localized patching technique subjected only isolated regions to metal deposition, the global metallization experiment exposed the NEMS and its surroundings to palladium deposition. While the system clearly remains intact, curling and increased bending of the nanowires is observed and is attributed to the thermal expansion coefficient mismatch between palladium and silicon. The thermal coefficient of expansion of palladium is four times larger than that of silicon. During this post-processing step we also worked to ensure that the formation of a palladium-silicon silicide ( $\text{Pd}_2\text{Si}$ ) will not take place by maintaining the sample's surroundings during the deposition process at approximately  $\sim 100^\circ\text{C}$ , keeping the deposition time short and eliminating any post-deposition annealing steps. We further expect the formation of a silicide to be hindered the presence of the native oxide on the nanowires' surface [14,15]. The electrical properties of the NEMS were also evaluated following the global deposition process. The results are consistent with the results of the localized deposition approach. As seen in Fig. 7, the current carrying capacity of the NEMS increases nine-fold to approximately 46 pA under 1 V input and the trend continues

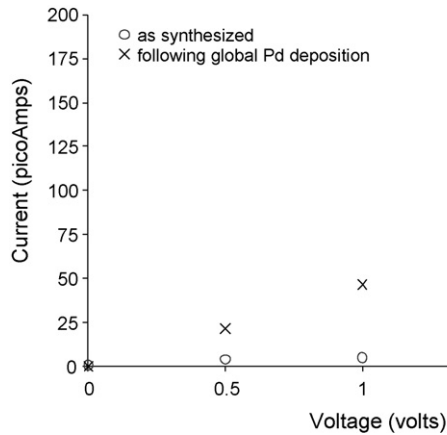


Fig. 7.  $I$ - $V$  characteristics of the NEMS before and after the global palladium metallization process.

with a 25-fold increase over the as-synthesized case to 150 pA under 2 V. The nonlinear behavior is noted in the  $I$ - $V$  curve, serving as an indication of the presence of non-ideal electrical properties.

It is difficult to make a fair direct performance comparison between the local deposition and global deposition approaches as the NEMS devices are different, the number of participating nanowires is vastly different, the deposited metal, deposition thickness and deposition methods are all different as well.

Next we tested the NEMS' performance in a functional application. Here we target a hydrogen sensing system realized by monitoring the resistance across the NEMS as hydrogen (100 ppm in  $N_2$ ) periodically enters a test chamber. This demonstration serves only as the proof-of-concept without benchmarking the state-of-art hydrogen sensors since intrinsic silicon nanowires impede sensor performance and as such are not suitable for hydrogen sensors. Based on thin film sensing mechanism, an increase in resistance is expected upon the exposure of a palladium film to hydrogen as the dissociation and diffusion of hydrogen onto the surface promotes increased scattering. Fig. 8 shows hydrogen sensing demonstration in terms of changes in resistance as a function of time upon the periodic exposure of

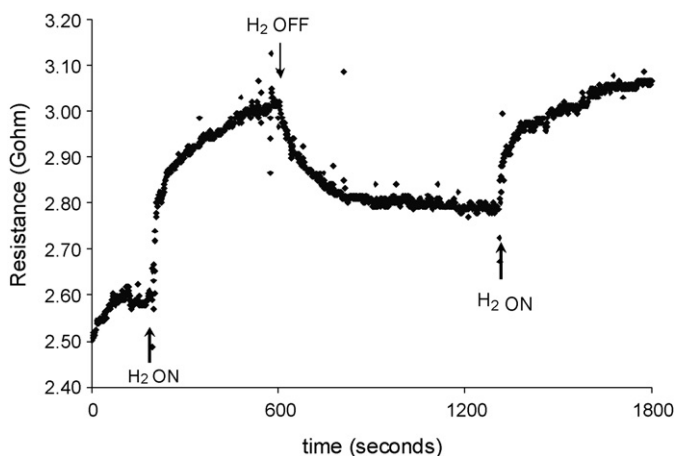


Fig. 8. NEMS sensor response in terms of the change in resistance as a function of time in a Pd functionalized NEMS upon periodic exposure to 100 ppm of  $H_2$ .

the system to hydrogen gas. Upon the initial exposure to  $H_2$ , the resistance across the system shows an instantaneous increase and then proceeds to increase at a slower rate. A gradual decrease in resistance is observed once the hydrogen flow is stopped. It appears that the system reaches a steady state resistance after approximately 5 min. With a subsequent exposure to  $H_2$ , we note an instantaneous change in resistance approximately half the magnitude of the initial resistance increase. The difference in the magnitude of the instantaneous resistance change is attributed to the poor reversibility of the sensor and possible fouling of the palladium film. Slightly elevated temperatures would ensure a better reaction surface and more consistent sensor response as reported for state-of-art hydrogen sensors. Further research will be required for silicon nanowire based hydrogen sensors.

In the third NEMS integrity test, the aqueous treatment experiments suggest that the system does maintain its structural integrity upon exposure to an aqueous environment and that the loss of contact occurs only during the drying process due to surface tension effects. The addition of a post-processing CPD step makes the system compatible with necessary aqueous functionalization environments and assists in maintaining the mechanical integrity of the system. In fact, our results show that over 95% of the original nano-to-micro contacts are present following the CPD step. We therefore confirm the effectiveness of the CPD process for the elimination of surface tension effects with nanoscale components. This experiment also highlights the asymmetry in our self-assembly method. Since it appears that the loss of contact to the bias structure occurs most often, we may deduce that the nano-to-micro contact at the growth structure yields a more robust mechanical bond than does the nano-to-micro contact at the bias structure. Synthesis conditions and specifically the local temperature are believed responsible for this behavior and could be adjusted to mitigate this shortcoming.

#### 4. Conclusions

Three post-processing techniques are used to examine the behavior, characteristics, and functionality of a self-assembled NEMS. This unique silicon nanowire based NEMS is found to be highly compatible with the conventional microscale processing techniques exercised here. Furthermore, the mechanical robustness of the system clearly stands out through the experiments while the hydrogen sensor demonstration illustrates a potential niche as well as a processing strategy for the NEMS at hand. In addition, we demonstrated an effective method for improving high contact resistance problems at the nano-to-micro interface. Finally, the importance of these experiments transcends beyond this specific silicon nanowire based NEMS as the use of post-processing techniques introduces a wide range of functional opportunities for NEMS integration and manufacturing.

#### Acknowledgments

This material is based upon work supported in part by the National Science Foundation under Grant No. EEC-0425914. We thank T. Yuzvinsky for assistance with the GIS system.

## References

- [1] A.M. Fennimore, T.D. Yuzvinsky, W.-Q. Han, M.S. Fuhrer, J. Cumings, A. Zettl, Rotational actuators based on carbon nanotubes, *Nature* 424 (2003) 408–411.
- [2] J.E. Jang, S.N. Cha, Y. Choi, G.A.J. Amaratunga, D.J. Kang, D.G. Hasko, J.E. Jung, J.M. Kim, Nanoelectromechanical switches with vertically aligned carbon nanotubes, *Appl. Phys. Lett.* 87 (2005) 163114.
- [3] O. Englander, D. Christensen, J. Kim, L. Lin, Post-processing techniques for the integration of silicon nanowires and MEMS, in: 19th IEEE International Conference on Micro Electro Mechanical Systems, Istanbul, Turkey, January 22–26, 2006, pp. 930–933.
- [4] O. Englander, D. Christensen, L. Lin, Local synthesis of silicon nanowires and carbon nanotubes on microbridges, *Appl. Phys. Lett.* 82 (2003) 4797–4799.
- [5] O. Englander, D. Christensen, J. Kim, L. Lin, S.J.S. Morris, Electric-field assisted growth and self-assembly of intrinsic silicon nanowires, *Nano Lett.* 5 (2005) 705–708.
- [6] Y. Cui, Z. Zhong, D. Wang, W.U. Wang, C.M. Lieber, High performance silicon nanowire field effect transistors, *Nano Lett.* 3 (2003) 149–152.
- [7] J. Hahn, C.M. Lieber, Direct ultrasensitive electrical detection of DNA and DNA sequence variations using nanowire nanosensors, *Nano Lett.* 4 (2004) 51–54.
- [8] G. Zheng, W. Lu, S. Jin, C.M. Lieber, Synthesis and fabrication of high-performance n-type silicon nanowire transistors, *Adv. Mater.* 16 (2004) 1890–1893.
- [9] S.E. Mohny, Y. Wang, M.A. Cabassi, K.K. Lew, S. Dey, J.M. Redwing, T.S. Mayer, Measuring the specific contact resistance of contacts to semiconductor nanowires, *Solid-State Electron.* 49 (2005) 227–232.
- [10] H.W.P. Koops, R. Weiel, D.P. Kern, T.H. Baum, High-resolution electron-beam induced deposition, *J. Vac. Sci. Technol. B* 6 (1988) 477–481.
- [11] A. Folch, J. Servat, J. Esteve, J. Tejada, M. Seco, High-vacuum versus “environmental” electron beam deposition, *J. Vac. Sci. Technol. B* 14 (1996) 2609–2614.
- [12] P. Huaptmann, *Sensors: Principles and Applications*, Prentice Hall International, Great Britain, 1993.
- [13] W.U. Wang, C. Chen, K. Lin, Y. Fang, C.M. Lieber, Label-free detection of small-molecule-protein interactions by using nanowire nanosensors, *PNAS* 102 (2005) 3208–3212.
- [14] R.W. Bower, D. Sigurd, R. Scott, Formation kinetics and structure of Pd<sub>2</sub>Si films on Si, *Solid-State Electron.* 16 (1973) 1461–1471.
- [15] R. Anton, Temperature dependence of Au–Pd thin film alloy contact formation on oxidized silicon substrates, *Thin Solid Films* 125 (1985) 305–311.

## Biographies

**Ongi Englander** holds a BS degree in mechanical engineering from the University of Maryland, and MS and PhD degrees in mechanical engineering from the University of California, Berkeley. Her research interests include micro-to-nano integration, nanostructure synthesis and the assembly of functional NEMS devices.

**Dane Christensen** received a BS in mechanical engineering from Rice University in 2001 and a PhD in mechanical engineering from University of California, Berkeley in 2005. His interests include mechanical application of nanomaterials and nano-composite structures.

**Jongbaeg Kim** received the BS degree in mechanical engineering from Yonsei University, Seoul, Korea, in 1997, the MS degree in mechanical engineering from the University of Texas, Austin, TX, in 1999, and the PhD degree in mechanical engineering from the University of California, Berkeley, in 2004. He was with DiCon Fiberoptics, Inc., Richmond, CA, from 2004 to 2005, where he designed and developed high-performance microactuators for telecommunication applications. He then joined the Yonsei University, where he is currently an assistant professor with the School of Mechanical Engineering. His research interests are mechatronic system dynamics, modeling, design and fabrication of MEMS, and nanotechnology.

**Liwei Lin** received the BS degree from National Tsing-Hua University, Taiwan, in 1986, and the MS and PhD degrees in mechanical engineering from the University of California, Berkeley (UC, Berkeley), in 1991 and 1993, respectively. He was with BEI Electronics Inc., USA, from 1993 to 1994 working in microsensors research and development. He was an associate professor with the Institute of Applied Mechanics, National Taiwan University, Taiwan, from 1994 to 1996, and an assistant professor with the Mechanical Engineering Department, University of Michigan, from 1996 to 1999. He joined UC, Berkeley, in 1999 and is now a professor with the Mechanical Engineering Department and is co-Director of the Berkeley Sensor and Actuator Center, an NSF/Industry/University Research Cooperative Center. His research interests are in design, modeling, and fabrication of micro/nanostructures, micro/nano sensors, and micro/nano actuators, as well as mechanical issues in micro/nano electromechanical systems. He holds eight U.S. patents. Dr. Lin is the recipient of the 1998 NSF CAREER Award for research in MEMS Packaging and the 1999 *ASME Journal of Heat Transfer* Best Paper Award for his work on micro scale bubble formation. He is a subject editor for the IEEE/ASME Journal of microelectromechanical systems and the North and South America Editor for *Sensors and Actuators A Physical*. He was the founding Chairman of the ASME MEMS division in 2004 and is a Fellow of the American Society of Mechanical Engineers (ASME).